

A Baldwin-favored Cyclization Inspires the Development of Fluorogenic Polymethine Dyes for Bioimaging

Annabell Martin^{§*} and Pablo Rivera Fuentes

[§]SCS-Metrohm Award for best oral presentation in Organic Chemistry

Abstract: Fluorescence imaging is an invaluable tool to study biological processes, and fluorogenic dyes are crucial to enhance cell permeability and target intracellular structures with high specificity. Polymethine dyes are vitally important fluorophores in single-molecule localization microscopy and *in vivo* imaging, but their use in live cells has been limited by high background fluorescence and low membrane permeability. Here, we present a general strategy to transform polymethine compounds into fluorogenic dyes by implementing a 5-*exo-trig* ring-closure. This method provides access to bright, fluorogenic polymethine dyes with emissions across the visible and near-infrared spectrum.

Keywords: Fluorogenicity · Live-cell microscopy · Polymethine dyes · Turn-on probes



Annabell Martin received her BSc and MSc in Chemistry from Heidelberg University. During this time, she carried out research stays abroad in the groups of Prof. Steven Ley and Prof. Ryan Shenvi, among others. In 2019, she joined the research group of Prof. Pablo Rivera-Fuentes (EPFL and UZH) for her PhD. Her research interests include the design of novel fluorogenic dyes and their application in bioimaging.

Parts of this article, including parts of Figs. 2–6, Schemes 3 and 5, have been published in open access form in ‘A General Strategy to Develop Fluorogenic Polymethine Dyes for Bioimaging’, A. Martin, P. Rivera-Fuentes, *Nat. Chem.* **2024**, *16*, 28, under a CC-BY license. <https://creativecommons.org/licenses/by/4.0/>

1. Introduction

Fluorescence imaging is a crucial technique to visualize many proteins simultaneously in living cells and study their structure, location, function, and trafficking. A common strategy to label a protein of interest (POI) is by fusing it to self-labeling proteins (SLPs), which can be tagged specifically with customized fluorescent dyes. SLPs combine the advantage of genetic encoding with the excellent brightness, tunability, and photostability of organic dyes. However, the use of synthetic dyes is often limited due to their low cell permeability and high background fluorescence.

1.1 Fluorogenic Dyes

The most successful dyes for SLP conjugation that overcome these challenges are fluorogenic. These dyes are non-fluorescent in solution but become highly fluorescent upon binding to their specific target (Scheme 1).

Over the last decade, several fluorogenic rhodamine dyes have been reported by leveraging the built-in cyclization equilibrium between a closed, non-fluorescent form and an open, fluorescent form. They have been used extensively in no-wash, multi-color,



Scheme 1. General fluorogenicity strategy.

live-cell imaging experiments,^[1,2] but unfortunately this rhodamine-based fluorogenicity strategy cannot be extended to the near-infrared (NIR) I (~750–900 nm) and II (~900–1700 nm) (Fig. 1A). The NIR I and II are crucial spectral windows for *in vivo* and tissue imaging due to the higher penetration depth, lower autofluorescence, and decreased phototoxicity compared to the visible range.

1.2 Polymethine Dyes

Polymethine dyes perform particularly well in the NIR because of their high extinction coefficients and short and simple synthesis (Fig. 1B). However, unlike rhodamine dyes, they do not possess a built-in intramolecular cyclization that could be leveraged to induce fluorogenicity. Previous attempts focused on the installation of nucleophilic side chains through the indoleninium nitrogen, but only resulted in pH-responsive dyes.^[3]

Here, we review our recently published design of efficient cyclizations for polymethine dyes and their use in bioimaging experiments.^[4]

2. Results and Discussion

2.1 Design of an Efficient Cyclization

An efficient fluorogenic dye suitable for live-cell imaging experiments must have a cyclization with a pK_a below 4 to ensure that the cyclic form is stable even in acidic vesicles. Cyclization reactions can be characterized using heuristic guidelines known as the Baldwin rules (Fig. 2A).^[5] We noticed that all previous attempts to create cyclizations in polymethine dyes were of the *endo-trig* type (Fig. 2B), whereas the ring-closure present in rhodamine dyes is of the *exo-trig* type (Fig. 2C).

We hypothesized that a Baldwin-favorable 5-*exo-trig* cyclization would also lead to robust fluorogenic polymethines. By changing the ring-closing nucleophile from the indoleninium nitrogen to the 3-position of the indolenine, the *endo* cyclization was converted into an *exo*

*Correspondence: A. Martin, E-mail: annabell.martin@chem.uzh.ch
Department of Chemistry, University of Zurich, CH-8057 Zurich

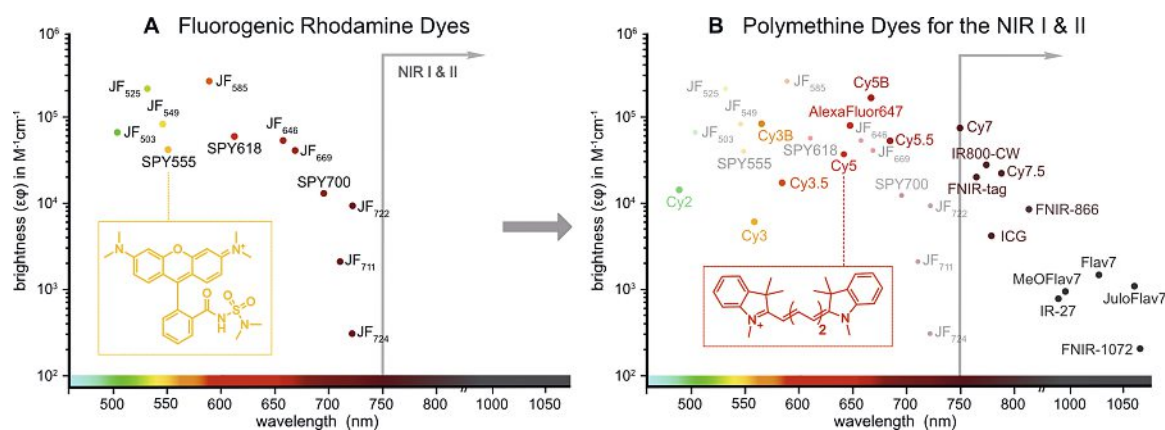


Fig. 1. Fluorophores for live-cell microscopy. A) Overview of fluorogenic rhodamine dyes, exemplified with the structure of SPY555. B) Polymethine dyes, here exemplified with the structure of Cy5, span the whole spectral range far into the NIR.

cyclization. Further stabilization of the closed form was envisioned with a CF_3 -substituent at the 5-position of the indolenine (Fig. 2D).

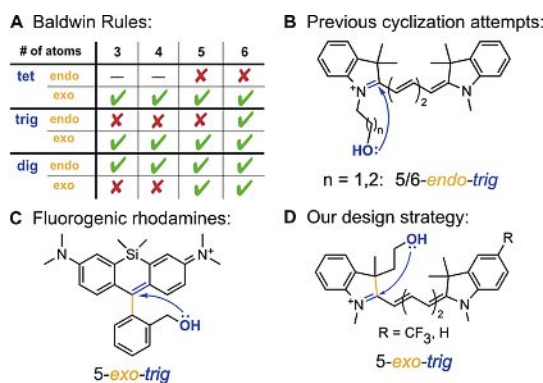
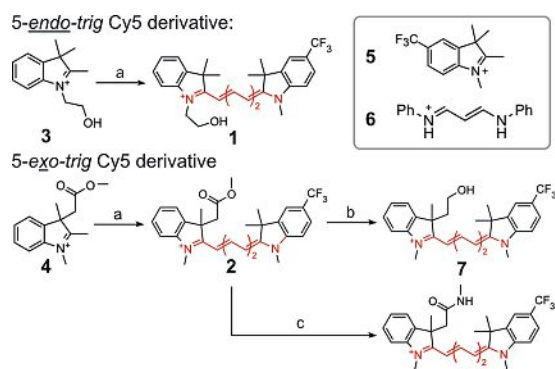


Fig. 2. A) Overview about the Baldwin Rules. B) Previous cyclizing polymethine dyes focused on *endo-trig* scaffolds. C) Rhodamine dyes possess a 5-*exo-trig* cyclization. D) Our fluorogenicity design involves a 5-*exo-trig* scaffold. Figure adapted from ref. [4].

2.2 Characterization of 5-*exo-trig* Cyclization

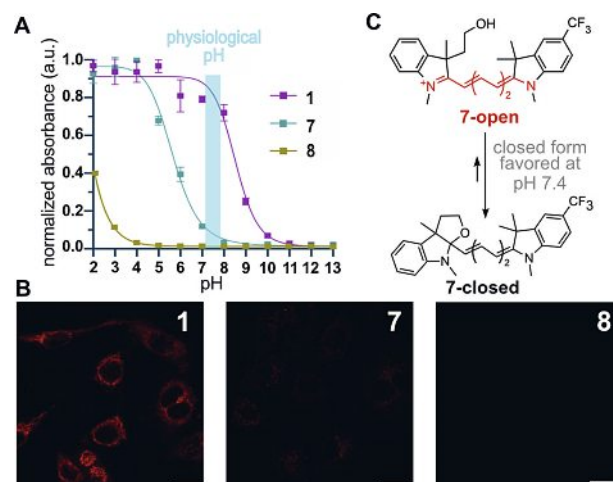
Cy5 derivatives **1** and **2** were synthesized in two-step microwave-assisted protocols using the simple indoleninium building blocks **3-5** and the linker **6** (Scheme 2). The cyclizing 5-*exo-trig* derivatives were obtained *via* methyl ester intermediate **2**, which was reduced to alcohol **7** and, to further diversify the nucleophiles, also transformed to N-methyl amide **8**.



Scheme 2. Synthesis of Cy5 derivatives. Reaction conditions for a: step1 **6**, Ac_2O , MW, 120°C , 1 h, step 2: **5**, pyridine, T, 30 min. T = 18°C for **1**, and T = 110°C for **2**; conditions for b: LiAlH_4 , THF, $0^\circ\text{C} \rightarrow 18^\circ\text{C}$, 16 h; conditions for c: CH_3NH_2 , THF, 66°C , 16 h. MW: microwave.

The cyclization efficiency was evaluated experimentally with pH titrations (Scheme 3A) and imaging experiments (Scheme 3B). The 5-*endo-trig* ring-closure present in **1** is not efficient as basic

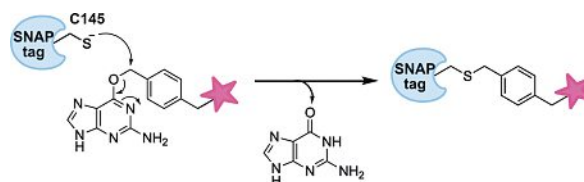
conditions are needed for cyclization, which is reflected in the high unspecific staining observed in live-cell imaging. The corresponding 5-*exo-trig* **7**, on the other hand, has a more efficient cyclization reaction (Scheme 3C) with a pK_a around 5.7, resulting in minimal background signal. Finally, the 5-*exo-trig* N-methyl amide **8** possesses a very efficient ring-closure with a pK_a below 2, and thus no fluorescence background signal. With this, we had successfully implemented a stable cyclization equilibrium in polymethine dyes.



Scheme 3. A) pH profiles of **1**, **7** and **8**. B) No-wash live-cell imaging of HeLa cells incubated with **1**, **7** and **8** (250 nM). C) Cyclization equilibrium of **7**. Figure adapted from ref. [4].

2.3 Turn-on with SNAP-tag

Next, we wanted to achieve a specific fluorescence turn-on and chose the SLP SNAP-tag^[6] to achieve this. SNAP-tag is derived from the human DNA repair protein O^6 -alkylguanine-DNA alkyl-transferase (hAGT). It recognizes 6-oxo alkylated benzyl-guanine (BG) motifs and irreversibly transfers the benzyl group to its active-site C145 residue (Scheme 4).



Scheme 4. Mechanism of SNAP-tag labeling.

Synthetically, the capping indoleninium was modified with an alkyne moiety for subsequent click reaction to an azide-modified BG substrate.

BG-compound **9** (Fig. 3A) exhibits a 10-fold turn-on in absorbance and 21-fold in fluorescence upon binding to purified SNAP-tag protein (Fig. 3B).

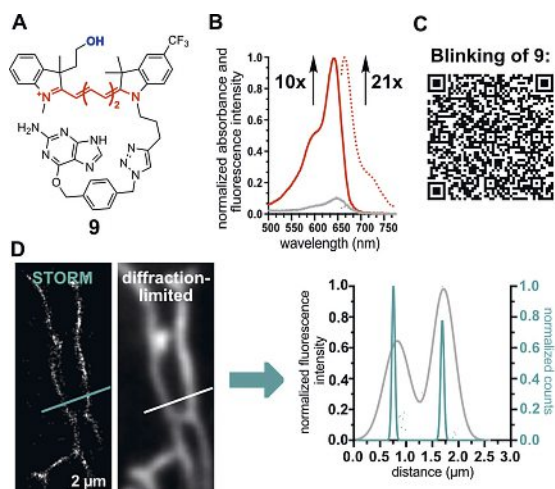


Fig. 3. A) Structure of **9**. B) *In vitro* turn-on of **9** with purified SNAP-tag protein. C) Movie of spontaneous blinking of **9**. D) Comparison between a super-resolved and a diffraction-limited image of tubulin structures of live HeLa cells incubated with **9** (100 nM). Figure adapted from ref. [4].

Moreover, this molecule is spontaneously blinking (Fig. 3C), making it suitable for live-cell single-molecule localization microscopy (Fig. 3D).

Next, we tested *N*-methyl amide Cy5-BG **10** (Fig. 4A) as a no-wash, fluorogenic Cy5 derivative. Compound **10** shows a 6-fold turn-on in absorbance and 19-fold in fluorescence upon binding to SNAP-tag protein (Fig. 4B). No-wash live-cell imaging experiments confirmed the specific fluorescence turn-on upon SNAP-tag binding in various organelles (Fig. 4C,D). In contrast, the Baldwin-disfavored *5-endo-trig* **11** (Fig. 4E) has a low turn-on upon SNAP-tag binding (Fig. 4F) and exhibits most of its fluorescent signal in vesicles, overshadowing the desired nucleus staining (Fig. 4G).

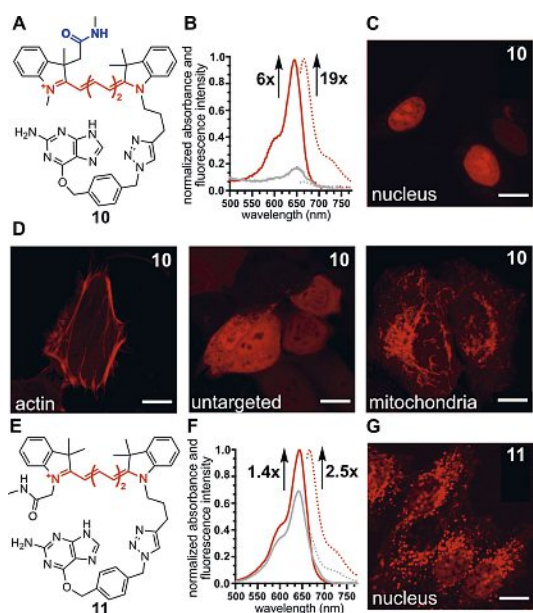


Fig. 4. A) Chemical structure of **10**. B) *In vitro* turn-on of **10** with purified SNAP-tag protein. C-D) HeLa cells were transfected with SNAP constructs targeting the indicated organelles and incubated with **10** (50 nM) for 2 h. E) Chemical structure of **11**. F) *In vitro* turn-on of **11** with purified SNAP-tag protein. G) HeLa cells were transfected with nucleus-targeted SNAP-tag and incubated with **11** (50 nM) for 2 h. Scale bar: 15 μ m. Figure adapted from ref. [4].

2.4 Expanding the Scope

Finally, we wanted to investigate the generality of this *5-exo-trig* ring-closing strategy for polymethine fluorogenicity. We first diversified the spectral range by varying the number of polymethine units, thus extending the spectral range to a yellow Cy3 ($n = 1$) and near-infrared Cy7 ($n = 3$). To balance the effects on the electrophilicity of the iminium carbon, fine-tuning with the ring-closing moiety and the 5-substituent at the indolenine was carried out.

We kept the electron-withdrawing CF_3 -substituent at the 5-position of Cy3-BG **12** to stabilize the closed form, thereby reducing background signal due to unspecific ring-opening while still achieving a good turn-on upon SNAP-tag binding (Fig. 5A-C). In case of Cy7-BG **13**, we installed an electron-deficient amide as ring-closing group to favor ring-opening, thereby increasing the turn-on while still maintaining low background signal (Fig. 5D-F).

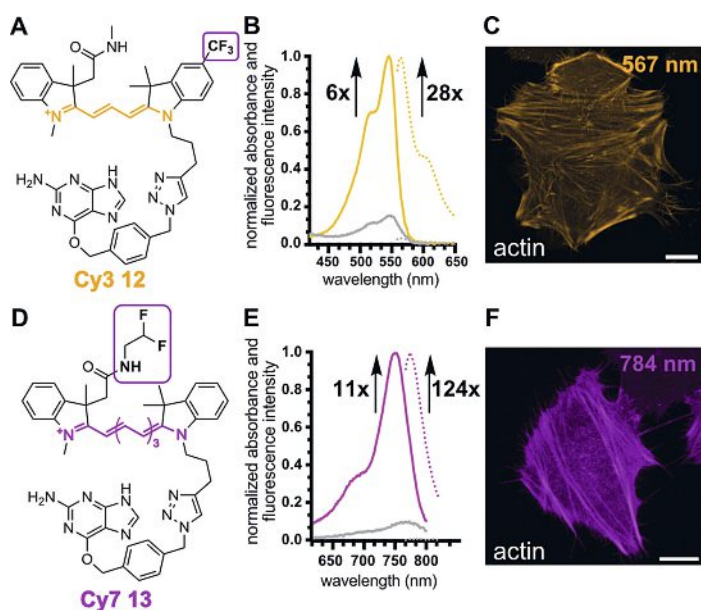


Fig. 5. A) Chemical structure of **12**. B) *In vitro* turn-on of **12** with purified SNAP-tag protein. C) HeLa cells were transfected with actin-targeted SNAP-tag and incubated with **12** (50 nM) for 2 h. D) Chemical structure of **13**. E) *In vitro* turn-on of **13** with purified SNAP-tag protein. F) HeLa cells were transfected with actin-targeted SNAP-tag and incubated with **13** (250 nM) for 2 h. Scale bar: 15 μ m. Figure adapted from ref. [4].

Next, we tested if ring-opening and subsequent fluorescence turn-on can also be achieved with different targets, such as the small-molecule ligand jasplakinolide,^[7] which binds to actin. Indeed, *N*-methyl amide Cy5 conjugated to jasplakinolide **14** (Fig. 6A) shows specific actin staining in live HeLa cells (Fig. 6B).

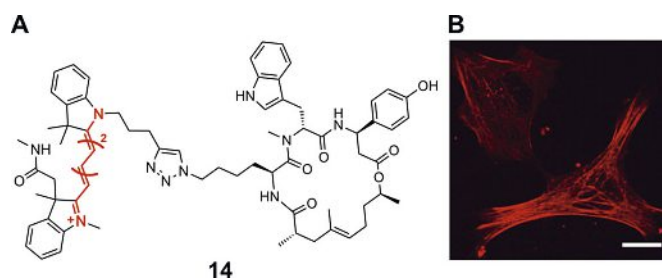
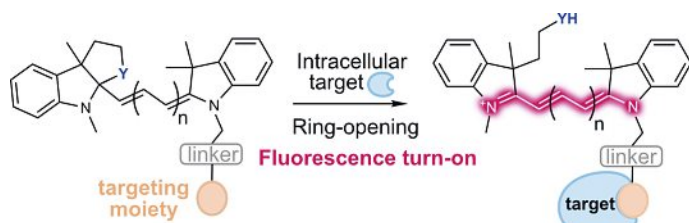


Fig. 6. A) Chemical structure of **14**. B) HeLa cells were incubated with **14** (250 nM) for 1 h. Scale bar: 15 μ m. Figure adapted from ref. [4].

3. Conclusions

In summary, we designed favorable cyclization reactions guided by the Baldwin rules, and incorporated this 5-*exo-trig* cyclization into the general dye scaffold of polymethine dyes. Only upon binding to their specific intracellular target, the ring opens up and renders the molecules fluorescent (Scheme 5).



Scheme 5. Overview about our fluorogenicity strategy. Figure adapted from ref. [4].

We have illustrated the generality of our turn-on scaffold by generating a spontaneously blinking Cy5 dye, and fluorogenic Cy3, Cy5, and Cy7 dyes.

Cy7 derivative **13** is particularly interesting because of its high brightness and long emission wavelength, making it suitable for *in vivo* imaging.

Furthermore, ring-opening and subsequent fluorescence turn-on can be achieved with self-labeling protein tags, such as SNAP-tag, as well as with small-molecule ligands, such as jasplakinolide.

We envision that our simple, yet general method, will be useful to develop improved fluorogenic probes particularly in the NIR, thereby facilitating new bioimaging experiments and creating novel chemigenetic sensors.

Acknowledgements

This work made use of infrastructure services provided by SCITAS, the Scientific IT and Application Support of EPFL, and S³IT, the Service and Support for Science IT at the University of Zurich. This work was funded by EPFL (SViPhD internal grant) and by the European Research Council (ERC Starting Grant HDPROBES, 801572).

Received: January 31, 2024

- [1] J. B. Grimm, B.P. English, J. Chen, J. P. Slaughter, Z. Zhang, A. Revyakin, R. Patel, J. J. Macklin, D. Normanno, R. H. Singer, T. Lionnet, L. D. Lavis, *Nat. Methods* **2015**, *12*, 244, <https://doi.org/10.1038/nmeth.3256>.
- [2] L. Wang, M. Tran, E. D'Este, J. Roberti, B. Koch, L. Xue, K. Johnsson, *Nat. Chem.* **2020**, *12*, 165, <https://doi.org/10.1038/s41557-019-0371-1>.
- [3] for selected examples see a) K. Miki, K. Kojima, K. Oride, H. Harada, A. Morinibu, K. Ohe, *Chem. Commun.* **2017**, *53*, 7792, <https://doi.org/10.1039/C7CC03035E>. b) M. Oe, K. Miki, H. Mu, H. Harada, A. Morinibu, K. Ohe, *Tetrahedron Lett.* **2018**, *59*, 3317, <https://doi.org/10.1016/j.tetlet.2018.07.044>. c) H. Mu, K. Miki, H. Harada, K. Tanaka, K. Nogita, K. Ohe, *ACS Sens.* **2021**, *6*, 123, <https://doi.org/10.1021/acssensors.0c01926>.
- [4] A. Martin, P. Rivera-Fuentes, *Nat. Chem.* **2024**, *16*, 28, <https://doi.org/10.1038/s41557-023-01367-y>.
- [5] J. Baldwin, *J. Chem. Soc. Chem. Commun.* **1976**, *18*, 734, <https://doi.org/10.1039/C39760000734>.
- [6] A. Keppler, S. Gendreizig, T. Gronemeyer, H. Pick, H. Vogel, K. Johnsson, *Nat. Biotechnol.* **2003**, *21*, 86, <https://doi.org/10.1038/nbt765>.
- [7] G. Lukinavičius, L. Reymond, E. D'Este, A. Masharina, F. Göttfert, H. Ta, A. Güther, M. Fournier, S. Rizzo, H. Waldmann, C. Blaukopf, C. Sommer, D.W. Gerlich, H.-D. Arndt, S.W. Hell, K. Johnsson, *Nat. Methods* **2014**, *11*, 731, <https://doi.org/10.1038/nmeth.2972>.

License and Terms



This is an Open Access article under the terms of the Creative Commons Attribution License CC BY 4.0. The material may not be used for commercial purposes.

The license is subject to the CHIMIA terms and conditions: (<https://chimia.ch/chimia/about>).

The definitive version of this article is the electronic one that can be found at <https://doi.org/10.2533/chimia.2024.196>